JOURNAL OF OPTOELECTRONICS AND ADVANCED MATERIALS Vol. 8, No. 4, August 2006, p. 1498 - 1501

The dielectric properties of laser-deposited $SrBi_2Ta_2O_9$ thin films and related buffer layers

D. MIU
National Institute for Laser, Plasma and Radiation Physics, P.O. Box MG-36, Bucharest, Romania

The electrical properties of pulsed laser deposited (PLD) oxide thin films were studied. The oxide materials were $SrBi_2Ta_2O_9$ (SBT), a material with ferroelectric properties, and related buffer layers for deposition onto silicon substrates, Yttria–stabilized zirconia (YSZ) and $SrZrO_3$ (SZO). YSZ films have a relative permittivity which depends on the thickness of the oxygen-deficient layer deposited immediately on top of the silicon substrate, and has values between 4 and 7. SZO has a large relative permittivity of 21, making it a high-k dielectric which is a potential replacement for SiO_2 as insulator in CMOS technology. The a-axis oriented SBT layer, however, has a very small memory window (about 80 mV), which could be due to intrinsic limitations of a-axis growth or to insufficiently optimized dielectric properties of the buffer layers.

(Received May 2, 2006; accepted July 20, 2006)

Keywords: Thin films, Ferroelectric, Fielectric properties, Laser deposition

1. Introduction

Oxides have extremely varied dielectric properties, ranging from insulators to superconductors, semiconductors, and ferroelectrics. This great variety of properties, as well as the compatibility of oxides with each other, makes them extremely attractive for various applications in microelectronics.

The research presented here was directed towards the study of the electrical properties of pulsed laser deposited (PLD) oxide thin films: $SrBi_2Ta_2O_9$ (SBT), Yttria-stabilized zirconia (YSZ; ZrO_2 stabilized with 9% Y_2O_3) and $SrZrO_3$ (SZO). Our main interest was SBT, a material with ferroelectric properties which is particularly promising for applications such as nonvolatile random access memories [1,2]. SBT presents a great advantage over the more commonly used PZT in that it does not suffer from the problem of fatigue, i.e. the gradual loss in polarization reversal with number of switches [3]. However, SBT also has a disadvantage, namely a pronounced structural anisotropy, which is reflected in a large anisotropy of its ferroelectric properties. The polarization of SBT is practically zero along the crystallographic c-axis, the easy polarization axis being oriented in the (a,b) plane [4]. It is therefore highly desirable to obtain epitaxial growth of SBT thin films with an in-plane c-axis. Since PLD normally leads to polycrystalline or c-axis growth of SBT [5,6], the study of buffer layers for the deposition of SBT was undertaken, in an attempt to promote a or b-axis growth.

YSZ is used as a first buffer layer deposited onto the silicon substrate, in order to remove the natural silicon dioxide layer, which is amorphous and does not allow epitaxial growth of thin films on top of it. SZO is used as an additional buffer layer, since SBT grown on top of the YSZ layer has poor ferroelectric properties even when complete SiO_2 removal is achieved. The dielectric properties of these buffer layers are important, since they determine the properties of the SBT/SZO/YSZ multilayers deposited on silicon.

SZO is also of great interest in itself, not just as a buffer layer, due to its high dielectric constant, which makes it a candidate for the replacement of SiO_2 [7], as well as for the fact that it can be switched between resistive states [8]. In this case, the dielectric properties of SZO/YSZ/Si substrates are also of interest in themselves.

2. Experiment

The thin film depositions were made using a Lambda Physik Compex 301 KrF laser (273 nm wavelength). The laser delivers an energy per pulse between 80 and 130 mJ; focusing of the beam using an optical system leads to an energy density of $1 \div 2$ J/cm^2 on the targets. Depositions were made onto p-type Si substrates placed 4 cm away from the target; doped Si was used in order to allow subsequent measurement of the dielectric properties of the films. The laser was operated at a repetition rate of 3 Hz. The substrates were heated to temperatures of $750 \div 850$ °C, depending on the material being deposited. Various oxygen pressures were used, as will be detailed later.

Analysis of the structure of the layers was made using X-ray diffraction (XRD). When necessary, in addition to θ - 2θ scans, φ scans were used to obtain more information on the in-plane epitaxy of the films. Low angle XRD scans were used to determine film thicknesses. More details on the XRD analysis is given in [9].

For the analysis of the dielectric properties, the capacitance-voltage (C-V) characteristics of the deposited films were measured using a Hewlett-Packard 4284A precision LCR meter, at a high frequency of 1 MHz. Prior to the measurement, the films were prepared by thermally evaporating gold pads for electrodes onto them using contact masks, without any subsequent thermal treatment; the diameter of the gold pads was 1 mm. Aluminum wires were then bonded to the pads, ensuring good electrical contact. The substrate was placed onto a copper support, to which it was glued using silver paste.

3. Dielectric properties of YSZ and SZO

The YSZ buffer layer has the role of removing the natural SiO_2 layer formed at the surface of the silicon substrate, which, being amorphous, prevents epitaxial growth of thin films. In order for this to occur, the conditions for the chemical reaction between the Zr in YSZ and the SiO_2 must be met. The first of these conditions is that the laser energy density on the YSZ target must be large enough to form the metallic zirconium necessary for the reaction, as opposed to zirconium dioxide; in our case this implied using a laser energy density of 1.5 J/cm^2. The second is that the deposition pressure must be low (below 6×10^{-6} mbar) to avoid gas-phase formation of zirconium dioxide from the ablated metallic zirconium. However, the low pressure condition is only for the first part of the YSZ film, since this is where the reduction reaction for silicon dioxide will occur; the rest of the layer must be deposited at a higher oxygen pressure (5×10^{-4} mbar was the optimum in our case) to ensure proper oxygen content and epitaxial growth. The thickness of the first, oxygen deficient layer, was varied between 0.8 and 1.7 nm. (To be more exact, this layer is oxygen deficient immediately after deposition; we have no information regarding any oxygen in-diffusion during subsequent deposition steps). The total thickness of the YSZ layer was typically 30 ÷ 40 nm when 1000 pulses were used for the deposition.

In the conditions mentioned above, a complete reaction of YSZ with SiO_2 occurred, and epitaxial c-axis growth of the YSZ layer was observed in the XRD figures. No dependence of these structural properties on the thickness of the oxygen-deficient layer was observed.

The dielectric properties of a typical YSZ film are illustrated in the C-V curve of Fig. 1. The film had an oxygen-deficient layer thickness of about 1.7 nm, and a total thickness of 30 nm (about 6% of the film is oxygen-deficient). The rest of the deposition conditions are the standard ones used by us for YSZ. The voltage range for the sweep was from –4 to + 4 V, and the step was 10 mV. The measurement was done at 1 MHz with an AC amplitude of 10 mV.

For negative bias voltages, the p-type semiconductor Si substrate is in accumulation and the only capacity measured is the capacity of the YSZ insulator. The same will be valid for the C-V curves of the SZO/YSZ and SBT/SZO/YSZ multilayer structures of insulator materials. From the value of the capacity in the accumulation regime, knowing the thickness of the film, the relative permittivity ε_r of the film material can be determined using:

$$C = \frac{\varepsilon_o \varepsilon_r S}{d} \quad (1)$$

where S is the surface of the electrodes (gold pads), which in our case is 0.8 mm^2, ε_0 is the permittivity of free space (8.85×10^{-12} F/m), and d is the film thickness. For the case of the YSZ film presented in Fig. 1, C is about 1.6 nF, which leads to a value of ε_r of about 7.

Fig. 1 also shows a shift in flat-band voltage between up- and down- sweep, which is called a memory window. In the case of the YSZ film in Fig. 1, the memory window is about 0.13 V.

The dielectric characteristics of YSZ are important because they determine the properties of the overlaying materials (SZO and SBT). In addition, the knowledge of the properties of YSZ alone is necessary in order to deduce the properties of the SZO and SBT thin films from the properties of the multilayers.

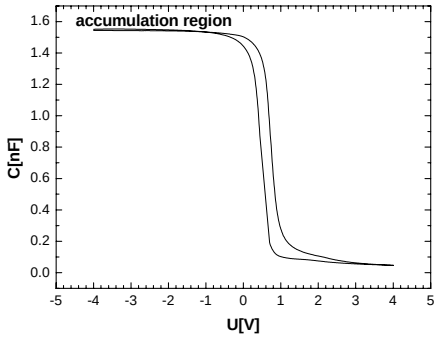

Fig. 1. Capacitance-Voltage curve for a YSZ film having a 1.7 nm oxygen deficient layer and a total thickness of 30 nm. The deposition conditions were standard for YSZ: deposition temperature 850 °C, laser pulse energy 100 mJ, oxygen pressure 5×10^{-4}mbar. The measurement was made at 1 MHz with a voltage step of 10 mV.

An important conclusion resulting from our measurements of the YSZ films is that YSZ with different thicknesses of the oxygen-deficient layers present a considerable difference in the dielectric properties, although the X-ray diffraction data indicates the same highly oriented c-axis films. Fig. 2 allows the comparison between a film having a 0.8 nm thick oxygen deficient layer out of a total of 40 nm (the oxide deficient layer represents about 2% of the total film thickness), and a film having a 1.7 nm oxygen deficient layer out of 30 nm (the oxide deficient layer is about 6% of the film thickness).

Using the data in Fig. 2, and the expression for the capacitance C used above, a value for the relative permittivity ε_r of 4 results for the 0.8 nm thick oxide deficient layer, and about 7 for the 1.7 nm thick oxygen deficient layer. The ε_r value of 4 coincides with that given in literature [10]. The conclusion is that ε_r is considerably larger for a larger oxygen deficient layer thickness. An additional difference that can be seen in Fig. 2 is that the film with the thinner oxygen deficient layer has a smaller shift from 0 V and a smaller hysterezis. A possible interpretation of this is the presence of less trapped charges for the less oxygen-deficient film, which leads to better film quality in this case.

In the case of SZO, the standard deposition conditions used of 5×10^{-4} mbar oxygen, 750 °C substrate temperature and 1 J/cm^2 laser energy density lead to highly a-axis oriented growth onto the YSZ buffer layers, as indicated by XRD [9]. A typical film thickness of 35 nm is attained for 1000 pulses. The SZO films have extremely

low surface roughness, as indicated by AFM. These results are very encouraging, considering that SZO presents a structural anisotropy, having both a and b axis lengths close to 5.8 Å, while the c axis has a constant of about 8.2 Å [11]. It is quite difficult to grow thin films having such a difference in axis length in the plane of the substrate surface.

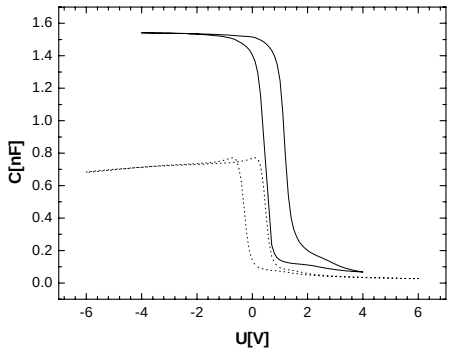

Fig. 2. Capacitance-voltage curve for YSZ films having: 1.7 nm thick oxygen deficient layer for a 30 nm total thickness of the film (full line); 0.8 nm thick oxygen deficient layer for a 40 nm total thickness of the film (dotted line). Standard YSZ deposition conditions. Measurement was made at 1 MHz with a voltage step of 0.1 V.

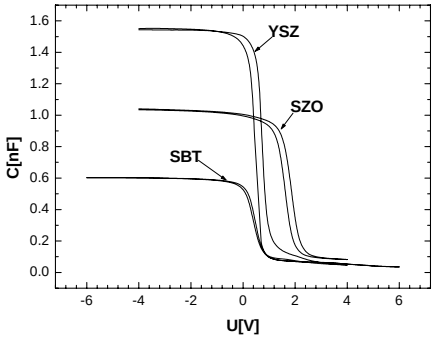

Fig. 3. Comparative C-V curves for a film consisting of only a YSZ layer (same conditions as figure 1), an SZO/YSZ film (SZO film in standard conditions) and an SBT/SZO/YSZ film. The SBT layer is deposited in 0.4 mbar oxygen, at an energy density of about 1.4 J/cm^2, and a deposition temperature of 800 ℃. All three YSZ layers, and the two SZO layers, are deposited in the same conditions for all three films given here. All of the films were measured with a 10 mV voltage step at 1 MHz.

The dielectric properties of SZO are illustrated in Fig. 3, where the curve for SZO corresponds to an SZO layer deposited in standard conditions on top of a YSZ buffer layer deposited in the same conditions as the YSZ/Si in Fig. 1. The relative permittivity ε_r of SZO can be found using the capacity in the accumulation regime of the SZO/YSZ multilayer, and considering that the SZO and YSZ layers are capacitors in series. For an SZO film thickness of 35 nm, an ε_r of 21 is obtained. This relative permittivity of SZO is large, making it a potential replacement for SiO_2 as an insulator in CMOS technology. At present, the ε_r of SiO_2 (=3.9) has become too low for the device sizes which will be reached in the near future. This will set a severe limitation on the development of microelectronic devices, whose miniaturisation has for decades followed Moore's law (which predicts the continuous downscaling of devices at an exponential rate) [12]. The ε_r of the SZO layers deposited in the experiments described here is comparable to that of $SrTiO_3$ (STO), STO being considered one of the most promising candidates for SiO_2 replacement [13]. The comparison is made for SZO and STO films having the same thickness, since for low thicknesses the film quality is degraded due to the poor properties of the interface, which become predominant. The value of ε_r for SZO is lower than the bulk value of 38; it is known that the value of ε_r is lower for materials in thin-film form compared to the value for bulk [14].

4. Dielectric properties of SBT

The SBT films were deposited at a deposition temperature of 800 °C. Various oxygen deposition pressures and laser energy densities were investigated; the domains investigated were 0.2 – 0.8 mbar for the pressure and 1 – 1.5 J/cm^2 for the target energy density. These two parameters proved decisive for the type of crystalline growth [15]. A-axis growth of SBT, which, as discussed, is more favorable for ferroelectric properties, is promoted by more energetic particles incident on the growing film surface. These energetic particles are produced for higher laser pulse energies and lower deposition pressures. θ - 2θ scans and evanescent-wave XRD analysis of the films show that approximately 25% of these films is a-axis oriented. The XRD results can be correlated with the surface morphology, as shown by SEM, in which a greater amount of a-axis material is associated with typical rectangular structures, similar to those observed by other authors [16]. The thickness of the film is typically 30 – 35 nm for 1000 pulses. After deposition, the trilayers were treated in-situ by cooling to about 250 °C in 30 min at the SBT deposition pressure. The chamber was then vented to atmospheric pressure and cooled to room temperature.

The dielectric properties of SBT/SZO/YSZ can be seen, in comparison to YSZ and SZO/YSZ, in Fig. 3. The SBT layer is deposited on top of YSZ and SZO obtained in the same conditions used for YSZ/Si substrates and SZO/YSZ/Si. From the total capacitance of the SBT/SZO/YSZ multilayer and the values for SZO/YSZ, a value for the ε_r of SBT of about 150 results; the value for bulk SBT at RT is about 180 [17].

The dielectric properties of the SBT film which, according to X-ray diffraction, is a-axis oriented, are poor, showing a very small memory window (about 80 mV). Although better dielectric properties were to be expected for a-oriented SBT films, these results could have more possible explanations. The first is that the underlying buffer layers do not have the optimum dielectric

properties, although the epitaxial growth is good, as we have already mentioned for YSZ. The second possibility is that the crystallite structure in the case of a-axis oriented SBT is such that the dielectric properties are poorer than one would expect from the large polarization along the a-axis. Our conclusion is that further research is needed to optimize the dielectric properties of the buffer layers, in order to obtain better dielectric properties of the ferroelectric films. One important point is the influence of the oxygen content of the layers upon the dielectric properties. This research would then clarify whether the poor dielectric properties of the SBT film are due to intrinsic limitations of a-axis growth or not.

5. Conclusions

Ferroelectric SBT films were laser-deposited onto buffered Si substrates. The buffer layers, YSZ and SZO, were also laser deposited, the YSZ immediately on top of the Si, and the SZO over the YSZ.

The deposition conditions used for YSZ ensured the complete removal of the native SiO_2 layer on Si and epitaxial c-axis growth of YSZ. Although the XRD data indicates the same high-quality epitaxial YSZ films for different thicknesses of the oxygen-deficient layers, these films present a cosiderable difference in dielectric properties. Films with a thinner oxygen deficient layer (2% of the total film thickness) have a relative permittivity ε_r of 4, which coincides with the value given by other authors. These films also have C-V curves with a smaller shift from 0 V and smaller hysteresis. Films with an oxygen deficient layer making up about 6 % of the total thickness have a higher ε_r of 7. A possible interpretation of this behaviour is that the less oxygen deficient film has less trapped charges, leading to a better dielectric film quality.

High quality SZO films are obtained on top of the YSZ. The films present highly-oriented a-axis growth, which is difficult to obtain since it implies considerable differences in the length of the axes in the plane of the substrate surface. The SZO films also have an extremely low surface roughness. A high dielectric constant of 21 is obtained for 35 nm thick SZO films. This implies that SZO has potential applications as a high-k material, a category of materials currently being intensively studied to replace SiO_2 as insulator in various microelectronic devices.

The SBT thin film growth is dependent on the energy of the particles incident on the growing film. The energy of the particles is dependent on the laser energy density on the target and on the deposition pressure, among other parameters. A higher energy of the particles (higher energy density or lower pressure) lead to a higher degree of a-axis growth (but not to 100%, in the deposition parameter domain used in the present experiments). This growth should be more favorable for the ferroelectric properties of SBT. However, the dielectric properties of our SBT films with a-axis orientation is poor, with a very small memory window.

Possible explanations for this are that the underlying buffer layers are not optimized from the point of view of the dielectric properties (which do not necessarily reflect the crystalline properties), or that the crystallite structure in a-oriented SBT leads to an intrinsic limitation of the polarization. Further research is needed to clarify the relationship between the dielectric properties and the deposition parameters (especially the oxygen content of the films), and for the optimization of the dielectric properties. For example, a higher a-axis content is obtained by increasing the energy of the incident species by decreasing the oxygen pressure, but this could also lead to poorer dielectric properties, as was observed in the case of YSZ. In this case, the increase of the energy of the incident species should be obtained in other ways, such as by increasing the laser pulse energy (to larger values than were investigated in the research presented here), or by means of other irradiation parameters we have not varied here, such as target-substrate distance or substrate temperature. Both of these parameters affect the energy of the species incident on the growing film.

References

[1] M. Takahashi, M. Noda, M. Okuyama, Jnl. Appl. Phys. **94**(3), 1912 (2003).
[2] H. N. Lee, D. Hesse, N. Zakharov, U. Goesele, Science **296**, 2006 (2002).
[3] S. B. Desu, D. P. Vijay, Mat. Sci. Eng. B **32**, 75 (1995).
[4] A. Gruverman, A. Pignolet, K. M. Satyalakshmi, M. Alexe, N. D. Zakharov, D. Hesse, Appl. Phys. Lett. **76**(1), 106 (2000).
[5] R. Dat, J. K. Lee, O. Auciello, A. I. Kingon, Appl. Phys. Lett **67**(4), 572 (1995).
[6] S. B. Desu, D. P. Vijay, X. Zhang, B. P. He, Appl. Phys. Lett. **69**(12), 1719 (1996).
[7] Z. Yu, R. Droopad, J. Ramdani, K. Eisenbeiser, Mater. Res. Soc. Symp. Proc **624**, 115 (2000).
[8] D. Halley, G. Norga, A. Guiller, J. Fompeyrine, J. P. Locquet, U. Dreschler, H. Siegwart, C. Rossel, Jnl. Appl. Phys. **94**(10), 6607 (2003).
[9] D. Miu, J.C. Martinez, M. Maier, H. Adrian, J. Optoelectron. Adv. Mater. **8**(1), 24 (2006).
[10] S. Ingebrandt, Dipl. Thesis, Universitaet Mainz, (1998).
[11] A. Ahtee, M. Ahtee, A. M. Glazer, A. W. Hewat, Acta Crystallographica Sect. B **320**, 3243 (1976).
[12] C. R. Foerst, C. R. Ashman, K. Schwarz, P. Bloechl, Nature **427**, 53 (2004).
[13] K. Eisenbeiser, J.M. Finder, Z. Yu, J. Ramdani, J. A. Curless, J.A. Hallmade, R. Droopad, W. J. Ooms, L. Salem, S. Bradshaw, C.D. Overgaard, Appl. Phys. Lett **76**(10), 1324 (2000).
[14] G. D. Wilk, R. M. Wallace, J. M. Anthony, Jnl. Appl. Phys **89**(10), 5243 (2001).
[15] Dana Miu, J.C. Martinez, L. Wiehl, R. Raitieri, H. Adrian, Materials Letters **59**, 1243 (2005).
[16] K. M. Satyalakshmi, M. Alexe, A. Pignolet, N. D. Zakharov, C. Harnagea, S. Senz, D. Hesse, Appl. Phys. Lett. **74**(4), 603 (1999).
[17] Landolt-Bornstein, Numerical Data and Functional Relationship in Science and Technology, New Series III/16a, Springer Verlag Berlin (1981).

*Corresponding author: miu@ifin.nipne.ro